

Nematicon-enhanced spontaneous symmetry breaking

A. Piccardi¹, A. Alberucci^{1,2}, N. Kravets¹, O. Buchnev³ and G. Assanto^{1,2,4}

1. NooEL - Nonlinear Optics and OptoElectronics Lab, University "Roma Tre", 00146 Rome, Italy
2. Optics Laboratory, Tampere University of Technology, 33101 Tampere, Finland
3. Optoelectronics Research Centre, University of Southampton, SO17 1BJ Southampton, UK
4. CNR-Institute for Complex Systems, 00185 Rome, Italy

Abstract: We investigate topological and optical spontaneous symmetry breaking in nematic liquid crystals subject to the Fréedericksz transition. Specular nematicon states couple to mirrored distributions of the director due to symmetry breaking, with transverse velocities controlled by beam power in the strong nonlinear regime. Hysteresis in transverse velocity versus incidence angle is observed in the soliton regime.

Keywords: spontaneous symmetry breaking, solitons, nonlinear optics, liquid crystals

Shortened Title: Nematicon SSB

Introduction

Nematic Liquid Crystals (NLC) are soft matter typically consisting of randomly positioned rod-like molecules with a high degree of orientational order [1]. When sandwiched in a finite size cell, NLC can acquire long-range orientational order through the alignment imposed by anchoring at the suitably treated surfaces of the cell. In this way the microscopic anisotropy of the constituent molecules can translate into a macroscopic homogeneous anisotropic response. Optically, a NLC slab usually behaves as a positive uniaxial crystal, with ordinary (n_{\perp}) and extraordinary (n_{\parallel}) refractive indices for electric fields perpendicular and parallel to the molecular director \mathbf{n} , respectively, the latter defining the optic axis [2]. Due to the tensorial nature of the relative permittivity, the Poynting vector \mathbf{S} of an optical beam will be angularly displaced with respect to its wavevector \mathbf{k} by the walk-off angle δ , depending on the angle θ between \mathbf{k} and \mathbf{n} through

$$\delta = \arctan\left(\frac{\varepsilon_a \sin^2 \theta}{\varepsilon_a + 2n_{\perp}^2 + \varepsilon_a \cos^2 \theta}\right)$$
 with $\varepsilon_a = n_{\parallel}^2 - n_{\perp}^2$ the optical anisotropy. Electric fields exert a

torque on the NLC molecular dipoles, $\Gamma = \varepsilon_a (\mathbf{n} \cdot \mathbf{E})(\mathbf{n} \times \mathbf{E})$, of strength depending on θ , such that the director tends to rotate towards the direction of the forcing field whenever the anisotropy is positive [2-3]. The electromagnetic torque is counteracted by the restoring elastic forces stemming from intermolecular interactions [1].

In case of an optical excitation with extraordinary polarization (an *e*-wave), molecular rotation translates into a net increase of the refractive index and, for a finite size beam, in self-focusing via the formation of a graded-index lens [2-4]. When self-action effects compensate for linear diffraction, the beam propagates with an invariant shape and profile, i.e., it becomes a (fundamental order) spatial soliton (SS) [5]. The intermolecular forces modify the index distribution with a “nonlocal” profile much wider than the beam itself, essentially limited by the size and geometry of the cell. The high degree of nonlocality allows the stabilization of (2+1)D SS in NLC [6] - named Nematicons [5] - otherwise unstable in local Kerr-like nonlinear media [7].

Nonlinear light beam propagation in NLC is therefore associated with a director distortion with respect to its rest distribution. A director reorientation modifies the local dielectric tensor, which in turn affects light propagation via Maxwell equations. Even when the director distortion is small with respect to the rest distribution, the dielectric changes correspond to a bell-shaped index deformation capable to guide the beam for powers of the order of a mW. When the distortion of the director distribution becomes comparable with the rest value, the beam trajectory starts to depend on the excitation via appreciable changes in walk-off [8]. Otherwise stated, light propagates in a non-perturbative nonlinear regime.

Spontaneous Symmetry Breaking (SSB) is ubiquitous in nature and occurs whenever the ground state of a system does not share the same symmetry of the Hamiltonian describing the system [9]. When SSB takes place, noise selects one of the outputs in a set of degenerate states. In NLC, topological SSB of the molecular distribution is possible due to the invariance of the director under π rotations (\mathbf{n} and $-\mathbf{n}$ are indistinguishable) [1] and is responsible for the formation of disclination lines, domain walls and defects in the director distribution [10-11]. In this Paper we discuss the simultaneous occurrence of optical and topological SSB in NLC in the highly nonlinear regime [12], addressing the role of light self-confinement and self-routing.

SSB under non-perturbative optical propagation

We refer to a planar NLC cell, as sketched in Fig.1. Planar anchoring at the two surfaces parallel to the plane yz forces the molecules to be parallel to the axis z . A third glass slide, perpendicular to the axis z and acting as an input interface, provides homeotropic alignment so that a uniform director distribution is available throughout the cell at rest. The input interface avoids the formation of a meniscus at the air/NLC interface, preventing uncontrollable lensing and beam depolarization [6].

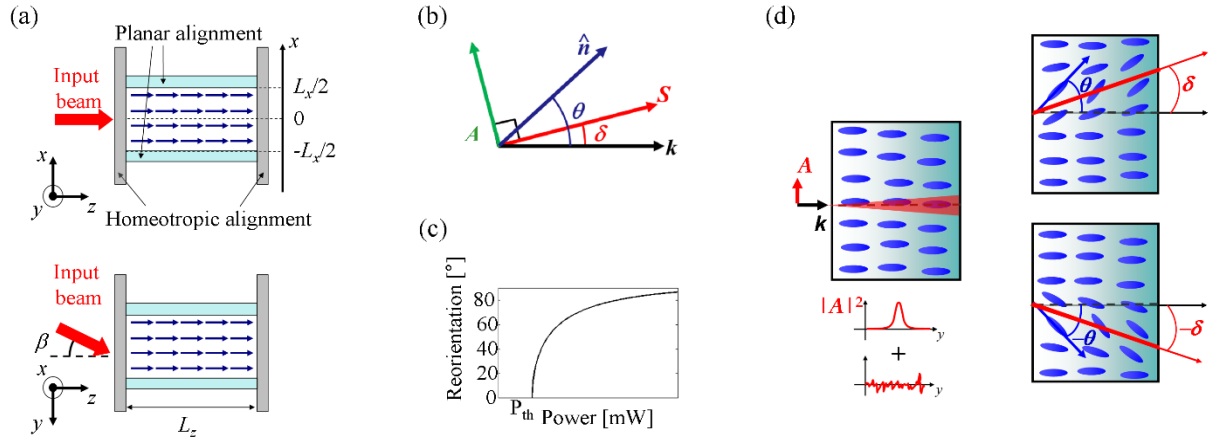


Fig.1 (a) Top (top) and side (bottom) view of the NLC cell. (b) Relevant vectors to describe extraordinary optical propagation in anisotropic uniaxial crystals. (c) When $\beta=0$ light-induced reorientation is inhibited below the threshold power defined by the Fréedericksz transition [3]. (d) Basic principle of entangled topological and optical SSB in NLC. The noise, either electromagnetic or in the molecular distribution, determines reorientation towards positive or negative y .

In the absence of illumination, the equilibrium state is expressed by $\nabla^2\theta = 0$, with boundary conditions determined by the anchoring at the glass/NLC interfaces. When a light beam impinges the sample, the reorientational equation reads [2, 5]:

$$\nabla^2\theta + \gamma \sin[2(\theta - \delta)] \left(|A|^2 - |\mathbf{E}_s|^2 \right) + 2\gamma \cos[2(\theta - \delta)] \text{Re}(\mathbf{E}_t \mathbf{E}_s^*) = 0 \quad (1)$$

where $\gamma = \varepsilon_0 \varepsilon_a / 4K$, with K the scalar Frank constant [1] and $\varepsilon_a = n_{\parallel}^2 - n_{\perp}^2$ the optical anisotropy.

The light electric field is given by:

$$\mathbf{E} = \mathbf{E}_t + \mathbf{E}_s = A(x, y, z) e^{ik_0 n_{\perp} z} \hat{t}(z) + \frac{i n_e \cos^2 \delta \partial_y A}{k_0 \varepsilon_{zz}} \hat{s}(z), \quad (2)$$

where A is proportional to the slowly varying envelope of the magnetic field. Subscripts t and s refer to the local direction of the electric field (for a plane wave with wave vector parallel to z) and of the Poynting vector, respectively, both of them changing with the director rotation (Fig. 1b) [8].

The propagation of such a field can be described by a nonlinear Schrödinger equation (NLSE):

$$\partial_z^2 A + 2ik_0 n_{\perp} \partial_z A + \partial_x^2 A + D_y \partial_y^2 A + k_0^2 \Delta n_e^2(\theta) A = 0 \quad (3)$$

where k_0 is the vacuum wave number, $\Delta n_e^2(\theta) = n_e^2(\theta) - n_\perp^2$ the nonlinear change in refractive index and $D_y = n_e^2(\theta)/\varepsilon_{zz}$ the diffraction coefficient along y .

We now consider an input beam with wave vector \mathbf{k}/z , polarized along y and focused on the input facet to a waist w_0 . In this situation, the electric field is normal to the director, thus the torque Γ is zero and Fréedericksz transition (FT) inhibits optical reorientation up to a threshold power P_{th} depending on the beam waist (Fig. 1(c)) [3].

When the FT is overcome, the electromagnetic torque can turn the fluctuations of the molecular order into a macroscopic rotation of the director, eventually enabling strong self-focusing [4] and self-guidance [5]. Given the NLC symmetry with respect to π rotations [1], the molecules can rotate to either positive or negative angles, the rotation direction (in the ideal case of perfect left/right symmetry) dictated solely by noise in the input beam and/or imperfections in the molecular distribution (Fig. 1d). In other words, SSB of the mirror symmetry with respect to the axis z takes place. In fact, according to Eqs. (1-3), the system is even symmetric with respect to z , but the final equilibrium state is not as the two available end-states for a fixed power mirror each other. Notably, while the sign of the walk-off angle derives from the sign of the molecular rotation and thus is dictated by noise, its magnitude is defined by the beam power, i.e., above FT the system is in the strong nonlinear regime [8]. Hence, topological SSB of the director distribution is inherently coupled to optical SSB of the beam propagation. Moreover, beam self-focusing with soliton formation enhance the whole phenomenon by increasing the torque.

Figure 2(a) shows simulated results from the coupled Eqs. (1-3) in a simplified (1+1)D geometry [12-13]. Random noise is superposed to the Gaussian beam at the input. Below FT no appreciable director rotation takes place and parity symmetry is conserved. When the input power is above the Fréedericksz threshold [3], optical and topological SSB manifest simultaneously, as sketched in Fig. 1(d).

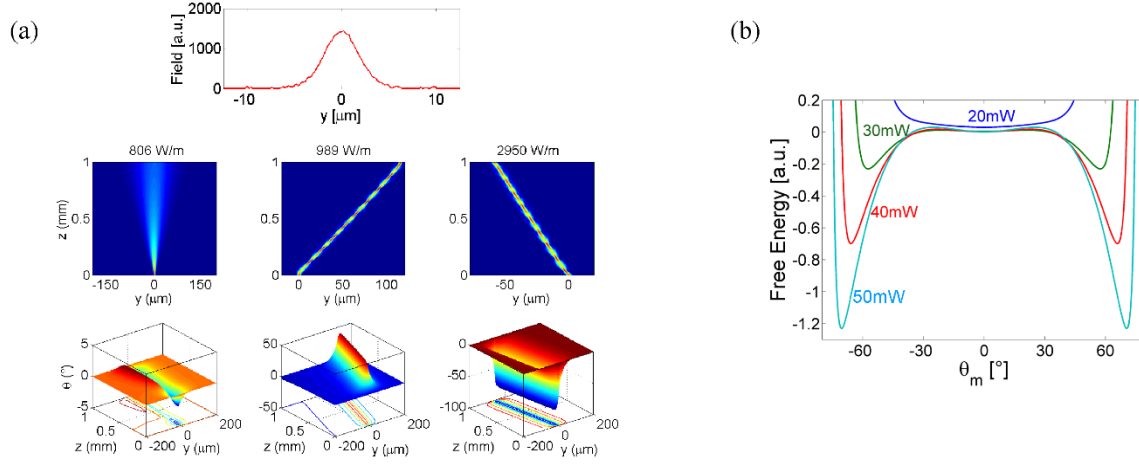


Fig. 2. (a) Numerical simulations of topological and optical SSB in NLC. Random noise (1%) is superposed to the input Gaussian beam. SSB leads to either positive or negative reorientation and walk-off, respectively, depending on the noise realization. (b) Free energy versus maximum reorientation as computed from Eq. (5) for various beam powers.

The overall free energy of the system permits to describe the observed phenomenon in terms of the so-called Mexican hat (“Sombrero”) potential, a standard model for SSB [9]. Under the single elastic constant approximation, the elastic energy is $F_{LC} = \frac{K}{2} \nabla \theta \cdot \nabla \theta$ and the electromagnetic energy is:

$$F_{opt} = -\frac{\epsilon_0}{2} \left[\epsilon_{\perp} \mathbf{E}^2 + \epsilon_a (\hat{n} \cdot \mathbf{E})^2 \right] + \frac{\mathbf{B}^2}{2\mu_0}, \quad (4)$$

with \mathbf{B} the magnetic field and μ_0 magnetic permeability.

For the sake of simplicity, we consider z -invariant beams, i.e., we neglect scattering losses [8] as well as soliton breathing [14] and longitudinal effects [15]. Under these approximations, the integration of the sum of the two energy terms yields [12]:

$$F = \frac{\alpha \kappa^2}{2} \theta_m + \frac{1}{2c} \left(\frac{n_{\perp}^2 - n_e^2(\theta_m)}{n_{\perp}} + \frac{4}{k_0^2 w_s^2} \right) P + \frac{\gamma Z_0 \sin[2(\theta_m - \delta_m)]}{4\pi c n_{\perp} \cos^2 \delta_m} \frac{dn_e}{d\theta} \Big|_{\theta=\theta_m} P^2 \quad (5)$$

where α and κ are two parameters dependent on material, geometry and beam waist [12], P is the beam power, c the speed of light in vacuum and Z_0 the vacuum impedance; the subscript m indicates

the values taken on the beam axis [12-13]. In the highly nonlocal limit, the soliton profile is Gaussian, with waist w_s [14].

The free energy versus the maximum rotation angle θ_m is plotted in Fig. 2(b). At low power optical reorientation is prevented and the only equilibrium position is the absolute minimum at rest ($\theta = 0$). Above FT, two minima appear symmetrically displaced with respect to $\theta = 0$, encompassing a power-dependent position and each of them corresponding to a stable soliton solution.

Experiments

We performed the experiments using the NLC cell as sketched in Fig.1, filled up with the commercial mixture E7 ($n_{\perp} \approx 1.5$, $n_{\parallel} \approx 1.7$ in the near-IR), with $L_x=100 \mu\text{m}$. A laser beam at $\lambda=1064\text{nm}$, with $w_0=8\mu\text{m}$, was injected into the cell via a microscope objective. The out-of plane scattered light was collected by a CCD camera in order to image the intensity evolution in the plane yz of the NLC layer.

To determine normal incidence with maximum accuracy, we maximized the power threshold required to trigger optical reorientation [4, 12]. We found that at normal incidence the minimum FT threshold was $P=30\text{mW}$. Due to the limited accuracy in determining the experimental parameters, the final states were probed by using deterministic sources of error, including non-orthogonal input alignment, asymmetric input profile and imperfect director anchoring. Moreover, above FT, domain formation with different reorientations was observed, leading to a wiggling beam trajectory. Fig. 3(a) shows an example of beam evolution above FT at normal incidence.

To overcome (or control) the deterministic errors, we followed the procedure sketched in Fig. 3(b). We biased the system by slightly tilting the incident beam at low power (tilt angle $<1^\circ$), so that $\theta \neq 0$. Then we increased the power to reach self-confinement [5]. Due to the small initial angle between the director and the wave vector, the beam underwent power-dependent negative refraction [16]. After equilibrium was reached, we realigned the wave vector parallel to z leaving the power

constant. The system kept memory of the reorientation and the beam propagated in the half-plane corresponding to the initial tilt (Fig. 4(a)). The dependence of resulting walk-off on input power is shown in Fig. 4(b). At low power the linear beam propagated straight along z ; above FT propagated along either of two symmetric paths with respect to z , the half-plane being determined by the initial tilt. The observed trajectories are not straight due to the scattering losses, which yield a power decay in propagation [8, 12]. The local slope of the path follows the walk-off dependence on reorientation [14, 17]: with reference to the section just after the input, the slope increased up to $P=70$ mW ($\theta=45$ degrees), then started to diminish for further increases in power.

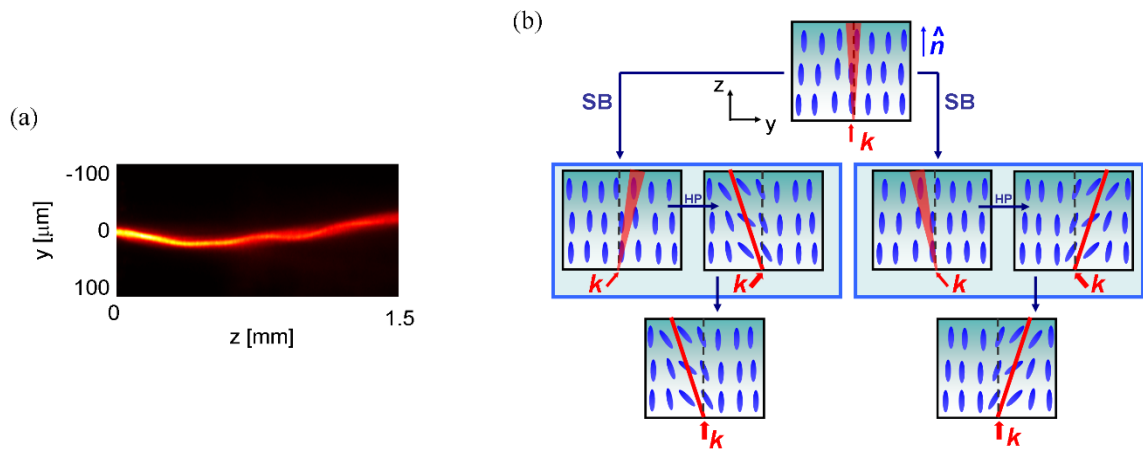


Fig. 3. (a) Acquired photograph of yz beam propagation above FT and with $\beta=0$. Domains form, resulting in a randomly warped trajectory. (b) Procedure to experimentally probe the SSB. At low power the beam is tilted, breaking the left-right symmetry, then the power is raised and eventually the beam is brought back to its initial direction. For the same input excitation, two regimes of propagation correspond to positive and negative walk-offs.

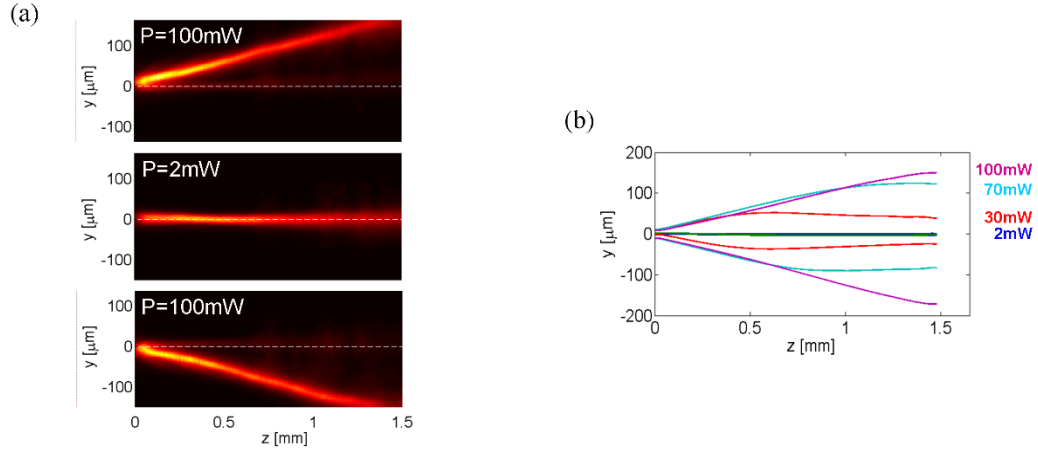


Fig. 4. (a) Acquired images of beam propagation in the plane yz . At low power the beam propagates along z (middle panel) conserving the initial symmetry. Once FT is overcome, SSB takes place and the beam can propagate indifferently in either of the two half-planes according to the initial tilt (see Fig. 3(b)). (b) Beam trajectories for various powers.

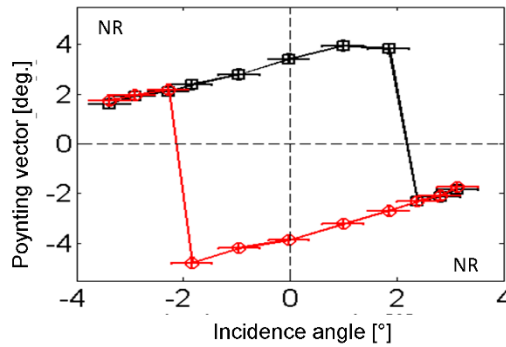


Fig. 5 Hysteresis cycle in soliton direction (Poynting vector angle) with respect to the incidence angle β . Black squares and red circles corresponds to increasing and decreasing input beam tilt, respectively. The beam power is 60mW.

The memory of the previous state should allow for the observation of hysteresis when the incidence angle is varied at a fixed input power, the latter above FT for normal incidence [18-19]. We launched an input beam tilted by about 4° with respect to the axis z . The input power was 60 mW in order to form a soliton. Under these conditions the beam was negatively refracted, its Poynting vector forming an angle of about -2° with z [12] (Fig. 5). When the incidence angle was gradually varied, the beam conserved a negative propagation angle up to normal incidence, thus undergoing

negative refraction. Once crossed normal incidence, the beam remained in the same half-plane, but undergoing positive refraction. When the incidence angle β reached about -2° , the beam trajectory abruptly jumped to negative refraction up to about 2° [12]. When the span of input wave vector was inverted, a specular dynamics could be observed. Thus, a hysteresis cycle controlled by the incidence angle was observed, in analogy to the position memory reported in Ref. [18] with reference to chiral NLC. All the acquired states were stable in time.

Conclusions and discussion

We reported on joint topological and optical spontaneous breaking of mirror symmetry in NLC. The phenomenon requires a configuration exhibiting the optical Fréedericksz threshold, where positive or negative reorientations of the molecules are energetically equivalent. We showed theoretically and confirmed numerically that the overall free energy shows two symmetric minima corresponding to positive or negative rotations. Experimentally, employing a set-up where light propagation within the NLC layer could be directly observed, we directly measure the sign of the director rotation, the latter determining the beam path via walk-off. Since at normal incidence deterministic errors dominated over stochastic noise, the presence of two symmetric states (topological and optical) was probed by tilting the input beam and then switching it back to normal incidence. Strong self-focusing and nematicon formation in the strong nonlinear regime enhanced the process, amplifying the torque acting on the molecular dipoles. Finally, we exploited the memory of the system to demonstrate a hysteresis cycle with respect to the incidence beam angle. Since spatial solitons in NLC are also light-induced waveguides, we envision potential applications in new generations of reconfigurable all-optical interconnects and devices.

Acknowledgements AA and GA thank the Academy of Finland for support through the FiDiPro grant no. 282858. The EU COST action IC 1208 is also gratefully acknowledged.

References

- [1] De Gennes, P. G. (1993). *The Physics of Liquid Crystals*. New York: Oxford Science.
- [2] Simoni, F. (1997). *Nonlinear Optical Properties of Liquid Crystals and Polymer Dispersed Liquid Crystals*. Singapore: World Scientific.
- [3] Durbin, S. D., Arakelian, S. M., & Shen, Y. R. (1981). Optical-field-induced birefringence and Freedericksz transition in a nematic liquid crystal. *Phys. Rev. Lett.*, *47*, 1411-1414.
- [4] Braun, E., Faucheux, L. P., & Libchaber, A. (1993). Strong self-focusing in nematic liquid crystals. *Phys. Rev. A*, *48*, 611-622.
- [5] Peccianti, M., & Assanto, G. (2012). Nematicons. *Phys. Rep.*, *516*, 147-208.
- [6] Peccianti, M., Conti, C., Assanto, G., De Luca, A., & Umetsu, C. (2004). Routing of anisotropic spatial solitons and modulational instability in nematic liquid crystals. *Nature*, *432*, 733.
- [7] Krolikowski, W. & Bang, O. (2010) *Solitons in nonlocal media: Exact solutions*, *Phys. Rev. A*. *63*, 016610
- [8] Piccardi, A., Alberucci, A., & Assanto, G. (2010). Soliton self-deflection via power-dependent walk-off. *Appl. Phys. Lett.*, *96*, 061105.
- [9] Nambu, Y. (2009). Nobel Lecture: Spontaneous symmetry breaking in particle physics: A case of cross fertilization. *Rev. Mod. Phys.*, *81*, 1015.
- [10] Nikkhou, M., Skarabot, M., Copar, S., Ravnik, M., Zumer, S., & Musevic, I. (2015). Light-controlled topological charge in a nematic liquid crystal. *Nat. Phys.*, *11*, 183-187.
- [11] Alexander, G. P., Gin-ge Chen, B., Matsumoto, E. A., & Kamien, R. D. (2012). Disclination loops, point defects, and all that in nematic liquid crystals. *Rev. Mod. Phys.*, *84*, 497-514.
- [12] Alberucci, A., Piccardi, A., Kravets, N., Buchnev, O., & Assanto, G. (2015). Soliton enhancement of spontaneous symmetry breaking. *Optica*, *2*, 783-789.
- [13] Alberucci, A., & Assanto, G. (2013). Modeling Nematicon Propagation. *Mol. Cryst. Liq. Cryst.*, *572*, 2-12.
- [14] Snyder, A. W., & Mitchell, D. J. (1997). Accessible solitons. *Science*, *276*, 1538-1541.
- [15] McLaughlin, D. W., Muraki, D. J., Shelley, M. J., & Wang, X. (1995). A paraxial model for optical self-focussing in a nematic liquid crystal. *Physica D*, *88*, 55-81.
- [16] Piccardi, A., Alberucci, A., Kravets, N., Buchnev, O., & Assanto, G. (2014). Power-controlled transition from standard to negative refraction in reorientational soft matter. *Nat. Commun.*, *5*, 5533-5541.
- [17] Alberucci, A., Piccardi, A., & Assanto, G. (2012). Tunable Nonlinearity in Nematicon Physics. *Mol. Cryst. Liq. Cryst.*, *558*, 2-11.
- [18] Beeckman, J., Madani, A., Vanbrabant, P. J., Henneaux, P., Gorza, S.-P., & Haelterman, M. (2011). Switching and intrinsic position bistability of soliton beams in chiral nematic liquid crystals. *Phys. Rev. A*, *83*, 033832.
- [19] Kravets, N., Piccardi, A., Alberucci, A., Buchnev, O., Kaczmarek, M. & Assanto, G. (2014). Bistable self-trapping with optical beams in a reorientational medium. *Phys. Rev. Lett.*, *113*, 023901.